HHS Public Access

Author manuscript

J Orthop Res. Author manuscript; available in PMC 2016 April 01.

Published in final edited form as:

J Orthop Res. 2015 April ; 33(4): 572–583. doi:10.1002/jor.22802.

Meniscus Tissue Engineering Using a Novel Combination of Electrospun Scaffolds and Human Meniscus Cells Embedded within an Extracellular Matrix Hydrogel

Jihye Baek, PhD[1,2], **Xian Chen, MS**[1], **Sujata Sovani, MS**[1], **Sungho Jin, PhD**[2], **Shawn P Grogan, PhD**[1], and **Darryl D D'Lima, MD, PhD**[1]

[1]Shiley Center for Orthopaedic Research and Education at Scripps Clinic, La Jolla, CA

[2]Department of Mechanical and Aerospace Engineering, University of California, San Diego, La Jolla, California

Abstract

Meniscus injury and degeneration have been linked to the development of secondary osteoarthritis (OA). Therapies that successfully repair or replace the meniscus are therefore likely to prevent or delay OA progression. We investigated the novel approach of building layers of aligned polylactic acid (PLA) electrospun (ES) scaffolds with human meniscus cells embedded in extracellular matrix (ECM) hydrogel to lead to formation of neotissues that resemble meniscus-like tissue. PLA ES scaffolds with randomly oriented or aligned fibers were seeded with human meniscus cells derived from vascular or avascular regions. Cell viability, cell morphology, and gene expression profiles were monitored via confocal microscopy, scanning electron microscopy (SEM), and real-time PCR, respectively. Seeded scaffolds were used to produce multilayered constructs and were examined via histology and immunohistochemistry. Morphology and mechanical properties of PLA scaffolds (with and without cells) were influenced by fiber direction of the scaffolds. Both PLA scaffolds supported meniscus tissue formation with increased COL1A1, SOX9, COMP, yet no difference in gene expression was found between random and aligned PLA scaffolds. Overall, ES materials, which possess mechanical strength of meniscus and can support neotissue formation, show potential for use in cell-based meniscus regeneration strategies.

Keywords

Meniscus; Electrospinning; Tissue Engineering; ECM Hydrogel

Corresponding Author: Darryl D. D'Lima, MD, PhD, Shiley Center for Orthopaedic Research and Education at Scripps Clinic, Scripps Health, 11025 North Torrey Pines Road, Suite 200, La Jolla, CA 92037, Tel 858 332 0166; Fax 858 332 0669, ddlima@scripps.edu.

AUTHOR CONTRIBUTIONS

JB, SPG, SJ and DDD were responsible for the overall experimental design. JB, SPG and DDD wrote the manuscript in close collaboration with the other authors. JB and SJ designed and conducted electrospinning and scanning electron microscopy. JB, XC, SS and SPG designed and conducted cell culture studies. SS and XC conducted RT-PCR and histology. All authors discussed the results and approved the final version of the manuscript.

COMPETING FINANCIAL INTERESTS STATEMENT

The authors declare no competing financial interests.

INTRODUCTION

Menisci are semilunar disc-shaped fibrocartilaginous tissues located on the tibial plateau. The major functions of this tissue include transmission of load and contribution to joint lubrication.[1] The menisci can be divided into outer and inner regions containing cells that are responsible for maintaining tissue homeostasis under the high shear and compressive forces experienced in the knee joint. The wedge shape of meniscus and its horn attachment serve to convert the vertical compressive tibiofemoral forces to horizontal hoop stresses. Simultaneously, shear forces are developed between the collagen fibers within the meniscus while the meniscus is deformed radially.[2] The outer region hosts blood vessels and is thus also termed the vascular region. Cells within the vascular region are mainly fibroblast-like and are elongated or spindle-shaped. The inner or avascular region is devoid of blood vessels and contains mainly chondrocyte-like cells that are rounded or spherical.[3]

Compromised meniscus function due to degeneration or injury is the most common risk factor for the development of knee osteoarthritis; the most common orthopaedic procedure is partial menisectomy, which also alters normal meniscus function.[4] Approximately 1.5 million arthroscopic surgical procedures of the knee are performed each year in the United States alone and of these more than half involve the meniscus.[5] Clinical interventions aim to preserve the meniscus structure and function. A number of techniques are being used to repair meniscal tears: polymer-based arrows, darts, screws, staples, and other suture devices.[6] However, because of the low probability of successfully repairing a torn meniscus, partial or total meniscus replacement is being actively developed.[7; 8]

To satisfy this need, a number of tissue engineering strategies have attempted to enhance the repair and replacement of damaged meniscus. Meniscus allograft transplantation has been explored as a solution to replace lost meniscal tissue to prevent cartilage degeneration, relieve pain, as well as to improve function.[9] Another approach is the direct replacement of meniscal tissue, in part or in whole, using natural or synthetic biomaterial scaffolds, including collagen-based grafts, subintestinal submucosa, cell-free hydrogels, degradable porous foams, multilayered, multiporous silk scaffolds and macro- and microporous polymeric meshes.[2; 10] Many of the above studies employing in vivo animal models or in human clinical trials show some chondroprotection by the implants but with a low success rate. With the exception of allografts, this failure is likely because the implants do not mimic the complex internal architecture and native mechanical properties as well as possess the appropriate resident cells.[11–14]

An alternative means to emulate meniscus nano- and microstructure with mechanical properties, and with high cell compatibility, may be achieved using a process called electrospinning. Electrospun scaffolds comprised of natural or synthetic materials in dimensions that mimic native collagen fiber bundles[2] can be efficiently produced by electrospinning.[15; 16] The combination of mechanical strength and biocompatibility qualities of electrospun nanofibers provide an advantage over other 3-dimensional (3-D) scaffolds using other techniques such as gas-foamed, salt-leached, freeform fabrication, topography library, and hydrogels. The high surface-to-volume ratio and porosity generated by the electrospun fibers facilitates cell attachment, cell proliferation, and transport of nutrients

through the scaffold.[17] A scaffold that provides the requisite mechanical properties of the meniscus may be useful for repair of meniscal tear defects and may permit early rehabilitation. Active joint motion during the early phase of repair also helps prevent restrictive adhesions and scar tissue formation that affect range of motion and limit recovery of function.[18]

In the past decade, biodegradable materials, such as polylactic acid (PLA) and poly(glycolic acid) (PGA), have been preferred especially in intra-articular procedures.[19] PLA has been more useful for biodegradable meniscal repair devices because the wet-strength half-life is 6 months.[20] The critical period for meniscal repair is 6 to 12 weeks[21] and PLA meniscal repair devices (e.g., Biostinger, meniscal screw, and meniscus arrow) preserve their initial strength even after six months.[22–24] Polylactides of varying molecular weights have been shown to be biocompatible,[25] Pure PLA has excellent mechanical properties including a tensile strength of 50 MPa and a modulus of 3.4 GPa.[26] The biocompatibility, suitable degradation time, and strength of PLA materials allow it to better mimic the structure, biological, and mechanical function of native extracellular matrix (ECM) proteins, which provide support and regulate tissue formation and regeneration.

In this study we aimed to: i) produce electrospun PLA scaffolds with random or aligned fiber arrangements similar to the collagen fiber arrangements in native meniscus,[27] which were examined for their mechanical properties and were observed under scanning electron microscopy (SEM); ii) examine the response of cultured human meniscus cells isolated from the vascular and avascular regions on these electrospun scaffolds in terms of cell viability, morphology and gene expression profiles; and iii) produce multilayered PLA constructs in an effort toward generating engineered meniscus-like graft tissue. These constructs were made by encapsulating human avascular meniscus cells in an extracellular matrix hydrogel sandwiched between layers of electrospun PLA. After culture, these engineered tissues were characterized by histology and immunohistochemistry to examine whether this approach would produce a meniscus-like tissue.

MATERIALS AND METHODS

Fabrication of poly lactic acid (PLA) scaffolds

PLA (Mw = 100,000, NatureWorks LLC, Minnetonka, MN) was dissolved in a mixed solvent of dichloromethane and N,N-dimethylacetamide (8/2 w/w) by stirring for 48 h at room temperature to obtain homogeneous 10 wt% solution. The PLA solution was loaded in a syringe, which was driven by a syringe pump (KDS200, KD Scientific Inc., Holliston, MA) at a feeding rate of 2.0 mL/h. A Teflon tube was used to connect the syringe and a 21G needle (inner diameter of 0.5 mm), which was set up horizontally. A voltage regulated DC power supply (NNC-30kV-2mA portable type, NanoNC, South Korea) was used to apply a voltage varying from 15 to 20 kV to the PLA solution to generate the polymer jet. The electrospun fibers were deposited in the form of a web on collectors covered by aluminum foil. For collecting random fibers, the tip-to-collector distance (TCD) was set to 16 cm on a flat plate as a collector. For collecting aligned fibers, a rotating drum (~2400 rpm) was placed at 12 cm from the tangent of the drum to the needle tip. To account for different collector sizes and effect of gravity, the TCD distances were optimized for the formation of

electrospun PLA fibers of consistent and of comparable diameter. An overview of the systems used to generate random and aligned electrospun scaffolds is shown in Figures 1A and 1B.

Structural morphology of PLA scaffolds

The morphology of electrospun PLA scaffolds was studied under scanning electron microscopy (SEM) (Philips XL30, FEI Co., Andover, MA) with an accelerating voltage of 10 kV. Scaffolds were coated with iridium using a sputter coater (Emitech K575X, EM Technologies Ltd, England). The diameter of individual electrospun fibers was measured from the SEM images using image processing software (Image J, National Institutes of Health, Bethesda, MD).

Tissues and cell isolation

Normal human menisci (medial and lateral) were obtained from tissue banks (with Scripps Institutional Review Board approval), from six donors (mean age: 29.8 ± 4.7; age range: 23–35 years; two females, four males). Normal menisci were selected following a previously reported macroscopic and histologic grading system.[28] The inner 2/3 (avascular region) and the outer 1/3 of the meniscus (vascular region) was separated with a scalpel and enzymatically digested using collagenase (2 mg/mL; C5138, Sigma-Aldrich, St. Louis, MO) in DMEM (Mediatech Inc, Manassas, VA) and 1% Penicillin-Streptomycin-Fungizone (Life Technologies, Carlsbad, CA) for 5–6 hours. The digested tissues were filtered through 100 μm cell strainers (BD Biosciences, San Jose, CA) and seeded in monolayer culture medium (MCM) consisting of DMEM (Mediatech) supplemented with 10% calf serum (Omega Scientific Inc. Tarzana, CA) and 1% Penicillin/Streptomycin/Gentamycin (Life Technologies). Cells were cultured for 1 passage before use in scaffold seeding experiments.

Cell cultures on single layered ES PLA scaffolds

Human cells from avascular or vascular regions of the meniscus were separately seeded onto 2 cm (length) × 1 cm (width) rectangular shape of random and aligned PLA scaffolds at a density of 0.5×10^6 per scaffold (0.25×10^6 per cm^2) in 6-well plates. Cells were cultured in DMEM supplemented with 10% calf serum and 1% Penicillin, Streptomycin, and Gentamycin for 3 days to permit cell attachment and scaffold colonization. Subsequently, the medium was changed to serum free ITS+ medium (Sigma-Aldrich) supplemented with 10 ng/mL TGFβ1 (PeproTech, Rocky Hill, NJ). The serum-free ITS+ medium used in ES scaffolds culture consisted of DMEM (Cellgro, Manassas, VA), 1 × ITS + (Sigma-Aldrich) (i.e. 10 mg ml^{-1} insulin 5.5 mg ml^{-1} transferrin, 5 ng ml^{-1} selenium, 0.5 mg ml^{-1} bovine serum albumin, 4.7 mg ml^{-1} linoleic acid), 1.25 mg ml^{-1} human serum albumin (Bayer, Leverkusen, Germany), 100 nM dexamethasone (Sigma-Aldrich), 0.1 mM ascorbic acid 2-phosphate (Sigma-Aldrich), and penicillin/streptomycin/gentamycin (Gibco, Carlsbad, CA).[29] After 2 weeks in culture with medium changes every 3 to 4 days, the cells on the scaffolds were assessed for cell viability by confocal microscopy and for cell morphology by histology and SEM.

Mechanical properties of PLA scaffolds

The mechanical properties of PLA scaffolds were quantified via tensile testing (n = 10 per group). Both random and aligned scaffolds were tested under three different conditions: i) freshly electrospun dry scaffolds were tested within 1 day of production; ii) scaffolds were seeded with avascular human meniscus cells and cultured for one and three weeks; and iii) scaffolds were cultured for one and three weeks without cells. For mechanical testing, the electrospun scaffolds were cut into dog-bone-shaped scaffolds using a custom-made aluminum template to guide reproducible testing shapes. The template was 50 mm in length, with a 5 mm width on each end and a central width of 2 mm (Figure 1D). The thickness of each scaffold was measured using a digital caliper and reported as mean ± standard deviation (SD). For mechanical testing of cultured cell-seeded and acellular scaffolds, human avascular cells (0.5×10^6 cells/each scaffold) were seeded on aligned PLA scaffolds. All cultures were in DMEM supplemented with 10% calf serum and 1% Penicillin, Streptomycin, and Gentamycin for 3 days to permit cell attachment and scaffold colonization. Subsequently, the medium was changed to serum-free ITS+ medium (Sigma-Aldrich) supplemented with 10 ng/mL TGFβ1 (PeproTech). After 1 week and 3 weeks in culture with medium changes every 3 to 4 days, the cell-seeded and non-seeded scaffolds were cut into the same dog-bone shaped specimens as the dry specimens and were evaluated for mechanical properties.

The specimens were mounted in the grips at their two ends of a uniaxial testing machine (Instron® Universal Testing Machine, 3342 Single Column Model; Norwood, MA) with a 500 N load cell and tested to failure at a crosshead speed of 1 mm min^{-1} at a gauge length of 20 cm under ambient conditions. Young's modulus was calculated from the slope of the linear segment of the stress-strain curve. Ultimate tensile strength (UTS) was calculated at the maximum load before failure. Values were presented as mean ± SD.

Multilayer construct formation

Human avascular meniscus cells (passage 1) were suspended in a hydrogel consisting of collagen type II (3 mg/mL), chondroitin sulfate (1 mg/mL) and hyaluronan (1 mg/mL) at 1×10^6 cells per mL. Cells suspended in hydrogel were seeded onto one aligned PLA scaffold (50 μL), followed by layering another scaffold sheet on top. Another cell layer was applied, followed by a final, third scaffold on the top (Fig. 1C). To stabilize the scaffold layers, a layer of 2% alginate (PRONOVA UP LVG; Novamatrix, Sandvika, Norway) was dispensed over the construct and crosslinked in calcium chloride (120 mM; Sigma-Aldrich) for 20 minutes. Layered constructs were cultured in serum-free medium supplemented with TGFβ1 (10 ng/mL).

Cell viability assessments

The viability of cells cultured on PLA scaffolds was observed using the live/dead kit consisting of Calcein-AM and Ethidium Homodimer-1 (Life Technologies) and a laser confocal microscope (LSM-510, Zeiss, Jena, Germany) as previously described.[30]

Cellular morphology of avascular meniscus cells on single layer PLA scaffolds

SEM was employed to observe high-resolution features of cells grown on the electrospun PLA scaffolds. After a culture time of 7 and 14 days, the cells on the substrates were washed with PBS and fixed with 2.5% weight/volume glutaraldehyde (Sigma-Aldrich) in PBS for 1 h. After fixation the samples were washed 3 times with PBS for 10 minutes each. The samples were then dehydrated in a graded series of ethanol (50%, 70%, and 90%) for 30 minutes each and left in 100% ethanol for 24 h at temperatures below 4° C. Next, the samples were kept in 100% ethanol until they were completely dried in a critical point dryer (Autosamdri-815, Series A, Tousimis Inc., Rockville, MD). The dried samples were then surface metalized by sputter coating with iridium for SEM examination. The morphology of the scaffolds and the adherent cells was observed by SEM (Philips XL30, FEI Co., Andover, MA).

Histology and immunohistochemistry

PLA scaffold layers seeded with avascular meniscus cells were fixed in Z-Fix (ANATECH, Battle Creek, MI) and embedded in paraffin. Sections of 5–7 μm were stained with H&E and Safranin O Fast Green. For detection of collagen type I by immunohistochemistry, cut sections were treated with hyaluronidase for 2 h,[31] and incubated with a primary antibody against collagen type I (clone: I-8H5; MP Biomedicals, Santa Ana, CA) at 10 μg/mL. For detection of collagen type II, (II-II6B3, Hybridoma Bank, University of Iowa) used at 10 μg/mL. Secondary antibody staining and detection procedures were followed as previously described.[32] An isotype control was used to monitor nonspecific staining.

RNA isolation and RT-PCR

Total RNA was isolated from single layer PLA constructs using the RNeasy mini kit (Qiagen, Hilden, Germany) and first strand cDNA was made according to the manufacturer's protocol (Applied Biosystems, Foster City, CA). Quantitative RT-PCR was performed using TaqMan® gene expression reagents. COL1A1, aggrecan, SOX9, COMP and GAPDH were detected using Assays-on-Demand™ primer/probe sets (Applied Biosystems). To normalize gene expression levels, GAPDH was employed using the ΔCt method.[33]

Statistical analysis

ANOVA and post-hoc student's t-test was used to assess the statistical significance of differences in fiber diameter, mechanical properties, and gene expression levels. P-values less than 0.05 were considered significant.

RESULTS

Controlled production of electrospun random and aligned PLA fibrous scaffolds

The morphological structures of aligned and random electrospun PLA fibers are shown in Figure 2. The rotating drum speed (~2400 rpm) and delivery parameters used produced scaffold structures with a high degree of alignment (Fig, 2B). The average diameter of aligned fibers was 1.25 ± 0.31 μm (range: 0.46–2.32 μm) and that for random PLA fibers

was 1.31 ± 0.56 μm (range, 0.70–3.84 μm). There was no statistically significant difference between the fiber diameters. Random scaffolds had a thickness of 0.15 ± 0.04 mm; the thickness of aligned scaffolds was 0.09 ± 0.03 mm.

Cell morphology and organization is dependent on PLA fiber orientations

Cells seeded upon randomly spun PLA scaffolds were flattened and spread-out with multi-directional extensions (Fig. 2C), while cells on aligned PLA scaffolds were elongated in line with the direction of the fibers (Fig. 2D). These differences in morphology and alignment were also reflected in the confocal images (Figs. 2E–F), which provided evidence of high cell viability for both scaffolds. No obvious differences in cell morphology were seen between the vascular or avascular cells.

Meniscus cell phenotype is not altered by fiber orientation or from region of isolation

In comparison to meniscal cells maintained in MCM (baseline control gene expression levels indicated by dotted line in Fig. 3), cells derived from either vascular and avascular regions cultivated on both random and aligned ES PLA scaffolds in serum-free ITS medium the presence of TGFβ1 (10 ng/ml) displayed significantly (p <0.05) increased COL1A1, SOX9 (Figs. 3A and 3B), and COMP (Fig. 3D) gene expression levels relative to monolayer cultured cells. Although decreased aggrecan mRNA was seen (approximately 2-fold) in cells on both scaffolds (Fig. 3C), this expression was not significantly different from the monolayer cultured cells.

High tensile mechanical properties of aligned electrospun PLA scaffolds

Young's modulus and UTS in the random and aligned scaffolds are presented in Figure 4. Random scaffolds possess an average tensile modulus of 67.31 ± 2.04 MPa. Aligned scaffolds, tested in the direction parallel to the aligned nanofibers generated a significantly greater (p < 0.001) tensile modulus of 322.42 ± 34.40 MPa, compared to random scaffolds. However, the tensile modulus perpendicular to the aligned direction was 7.18 ± 1.27 MPa, significantly weaker than random scaffolds (p < 0.001). Similarly, UTS of aligned scaffolds was significantly (p < 0.001) higher: 14.24 ± 1.45 MPa (parallel to direction of alignment) compared to 3.8 ± 0.21 MPa measured in the random ES scaffolds.

Random and aligned scaffolds tested in the direction of fiber orientation generated a sharper increase in stress with a "toe region" in the pre-yield region. While random scaffolds extended nonlinearly after yield, aligned scaffolds generated crack straining (Figs. 4C–E), yielded, and failed at comparatively adjacent points earlier in the strain region. Aligned scaffolds measured in the direction perpendicular to fiber orientation, exhibiting a much lower stress-strain response (Figs. 4C and 4F).

Mechanical properties of cell-seeded and paired acellular scaffolds were assessed over time in culture via tensile testing. The stiffness of all scaffolds showed some decrease with time in culture. However, cell-seeded scaffolds tended to possess higher stiffness and reached a higher ultimate tensile stress, although no significant difference was established.

Multi-layer PLA cell-seeded scaffold support meniscus-like neotissue formation

Since the random PLA scaffolds yielded a much lower average tensile modulus (67 MPa) than the aligned scaffolds (>300 MPa), we chose to make multilayers of scaffolds using only aligned fibers to mimic the circumferential collagen fibrous bundles in native meniscus. Human avascular meniscus cells were seeded onto three scaffolds within a biomimetic gel composed of collagen type II, chondroitin sulfate and hyaluronan (1 mg/mL each) and held in place with a layer of 2% alginate crosslinked with calcium chloride (Fig. 1C). Following 2 weeks of culture, a construct was developed that comprised of a fusion of the PLA scaffold layers, newly synthesized ECM and cells that had infiltrated and distributed inside and throughout the triple-layered construct (Figs. 5A–F). The neotissue was Safranin-O negative (Figs 5A and 5B), and possessed an ECM composed of collagen type I (Fig. 5C) and with cells elongated in the same direction/orientation as the ES PLA fibers. Immunostaining for collagen type II was negative for these neotissues (data not shown).

DISCUSSION

The ultrastructural arrangement of collagen fibers in the superficial and laminar layers of the meniscus comprises of random collagen fibers. However, the main central layer is made up of circumferentially aligned collagen bundles that are critical for the mechanical function of the meniscus.[27] We demonstrated the capacity to create both random and aligned electrospun scaffolds, which resemble the architecture of the native meniscus, by using electrospinning technology. We investigated the potential of combining human meniscus cells with nanofibrous scaffolds for meniscus tissue engineering. These electrospun PLA scaffolds possessed anisotropic mechanical properties, mimicked the native central layer of the meniscus tissue (the main bulk of meniscus tissue consisting of collagen fibrils[27]), and supported cell growth to permit production of the major ECM components seen in meniscus tissue. Our data also show that electrospinning can be employed in conjunction with a novel cell-seeded biomimetic hydrogel to produce higher order constructs that promote neotissue formation and scaffold integration. These results demonstrate proof of concept of using such scaffolds for meniscus tissue engineering.

Production of scaffolds via electrospinning has been carried out with numerous synthetic polymers including polyurethanes, PLA, poly-ε-caprolactone (PCL), and polydioxanone. The attachment and proliferation of cells, deposition of matrix, and the development of mechanical properties of the scaffolds over time is highly dependent on the type of material.[34] The initial high strength and relatively long degradation time of PLA helps to mimic the structure and biological function of native ECM proteins, which may support the formation and maturation of the tissue.

However, the initial mechanical properties of scaffold are important for implant survival before eventual replacement and remodeling of regenerated tissue. We established that the tensile modulus of aligned scaffolds was approximately 5-fold higher than randomly oriented scaffolds and was comparable to the high end of the tensile modulus of human meniscus in the circumferential direction. The pronounced ‘toe’ region seen in the stress-strain curve of circumferential parts of meniscus was also seen in ES aligned PLA scaffolds in the present study (Figs. 4C and 4E).

The mechanical properties of our PLA scaffolds were significantly higher than those reported elsewhere for aligned nanofiber scaffolds.[35–37] For example, random PCL scaffolds had an isotropic tensile modulus of 2.1 ± 0.4 MPa, compared to highly anisotropic PCL scaffolds whose modulus was 11.6 ± 3.1 MPa in the presumed fiber direction.[35] To increase mechanical strength of electrospun PLA, Seth et al,[38] produced randomly electrospun nanocomposite scaffolds by encapsulating multi-walled carbon nanotubes (MWNT) in PLA. The combined PLA and MWNT increased the modulus of the randomly oriented electrospun scaffolds to 55 MPa.[38] However, this modulus is in the low end of the range of moduli reported for human menisci, and even lower than the tensile properties of the randomly oriented scaffolds reported in the present study.

Electrospun nanofibers (50–1000 nm) are similar in diameter to the native extracellular matrix.[39] This nano-sized fiber diameter has been shown to promote matrix-forming activities in seeded cells, for instance, chondrocytes seeded on PLLA nanofibers produce more matrix than when seeded on PLLA microfibers.[40] We therefore focused on the generation of engineered meniscus constructs using nanofibrous biodegradable scaffolds produced via electrospinning in this range (nominally 500–1000 nm). Human meniscus cells infiltrated and distributed within aligned electrospun scaffolds with an elongated morphology resembling cells in native meniscal tissue. We also observed the production of ECM with high collagen type I content by human meniscus cells between the PLA fibers and throughout the multiple electrospun PLA layers within 14 days of culture. The low GAG staining is also consistent with normal human meniscus.[28]

Notably, fiber orientation affected the morphology of cells on these scaffolds. Meniscus cells seeded on random PLA scaffolds were flattened with multi-directional extensions, while they were more elongated and in line with the direction of the fibers on the aligned PLA scaffolds. In this current study, both random and aligned scaffolds induced meniscus-like gene expression profiles as previously reported.[41; 42] Despite differences in the observed cell morphology and in the observed via confocal and SEM images, we could not detect significant differences in gene expression due to fiber alignment, cell morphology, or due to region of origin (vascular or avascular). This result was likely because in both cases, the cell morphology remained fibroblast-like. Similar to our study with human meniscus cells, others have also reported that bovine meniscus fibrochondrocytes or bovine mesenchymal stem cells derived from bone marrow preferentially aligned in the predominant fiber direction, whereas cells on nonaligned scaffolds were randomly oriented.[15] In addition, Baker et al [15] noted a significant increase in mechanical properties after 70 days for aligned PCL scaffolds compared to random constructs seeded with either cell type. In this current study, the mechanical properties of cell-seeded scaffolds were higher than non-cell seeded scaffolds at every time point. Importantly, this indicates that these improvements in mechanical property can be attributed to the neotissue deposited by the cells on each scaffold.

Hydrogels consist of entangled polymer chains that have an amorphous to semi-fibrous character, whereas ES scaffolds display distinct nano- to microscale topography that can be easily tuned.[43] Hydrogels reinforced with nanofibers are therefore an attractive approach to tissue engineering since nanofibers can enhance the poor mechanical properties of

hydrogels. One study used a blend of PCL and gelatin but only reported a compressive strength of about 20 kPa.[44] Synthetically reinforced hydrogel-electrospun scaffold composite materials improved cell proliferation, and attachment and spreading of neuroblastoma and rat cortical neuron cells that was attributed to the topography of the electrospun fibers.[44; 45] We used a different approach to assemble nanofibrous scaffolds into complex architectures by stacking multiple layers of fibers sequentially deposited on top of one another (~1.5 mm total thickness) for proof-of-concept engineering of fiber-reinforced meniscal tissues. The motivation for developing multilayered constructs was to mimic regions of native tissue with respect to its biochemical, structural, and mechanical properties at a clinically relevant scale.[42; 46] Combining electrospinning with a biomimetic gel also provided cells with a growth environment to support neotissue development similar to the ECM found in native avascular meniscus tissue and aided in fusing multiple layers together. Although cells typically spread out on the surface of electrospun scaffolds, these cells also infiltrated inside each of the PLA scaffold layers.

Several issues remain to be addressed in the production of a functional construct for meniscus repair. While PLA is an FDA-approved biomaterial and is widely used clinically, resorbed PLA scaffolds can lead to synovitis and chondral lesions.[22; 23] Hence, a natural scaffold or more biocompatible material with nonreactive degradation products is more desirable. Since only one group was studied, we could not test specific hypotheses about the impact of the various components of the constructs. Assays of biochemical composition are also important to assess potential for clinical translation. We did not test the delamination strength of layered constructs due to technical challenges. While our primary intention in the present study was to demonstrate proof of concept with respect to biocompatibility, meniscal cell phenotype, and neotissue formation, in future studies we aim to test whether these constructs can be used to repair defects created in an ex vivo tissue model.

In summary, we electrospun PLA to generate biodegradable and biomimetic nanofibrous scaffolds. Aligned electrospun PLA fibers generated an anisotropic tensile modulus that better approximated the properties of meniscal tissue than random electrospun PLA fibers. Cells from avascular and vascular regions of human menisci survived, attached, and infiltrated the PLA nanofibrous scaffold, and secreted the major proteins found in meniscal matrix. Moreover, we were also able to demonstrate the novel approach of combining nanofibrous scaffolds with human meniscus cells in an ECM hydrogel to create thicker multilayered constructs in the dimensions necessary for partial meniscus replacement.

Acknowledgments

Funding provided by California Institute of Regenerative Medicine (TR1-01216), National Institutes of Health (P01 AG007996); The Scripps Translational Science Institute (UL1 RR025774), the UC Discovery Grant (ele08-128656/Jin) and by the National Science Foundation (DMR-1006081). We greatly appreciate assistance by Christine Frandsen (SEM cell imaging) and Judy Blake (manuscript formatting and copyediting).

References

1. Ghosh P, Taylor T. The knee joint meniscus: a fibrocartilage of some distinction. Clin Orthop Relat Res. 1987; 224:52–63. [PubMed: 3311520]

2. Makris EA, Hadidi P, Athanasiou KA. The knee meniscus: structure-function, pathophysiology, current repair techniques, and prospects for regeneration. Biomaterials. 2011; 32:7411–7431. [PubMed: 21764438]
3. McDevitt CA, Mukherjee S, Kambic H, et al. Emerging concepts of the cell biology of the meniscus. Curr Opin Orthop. 2002; 13:345–350.
4. Katz JN, Martin SD. Meniscus--friend or foe: epidemiologic observations and surgical implications. Arthritis Rheum. 2009; 60:633–635. [PubMed: 19248081]
5. Rodkey WG, Steadman JR, Li S-T. A clinical study of collagen meniscus implants to restore the injured meniscus. Clin Orthop Relat Res. 1999; 367S:S281–S292. [PubMed: 10546653]
6. Lozano J, Ma C, Cannon W. All-inside meniscus repair: a systematic review. Clin Orthop Relat Res. 2007; 455:134–141. [PubMed: 17179785]
7. Englund M, Roos EM, Lohmander LS. Impact of type of meniscal tear on radiographic and symptomatic knee osteoarthritis: a sixteen-year followup of meniscectomy with matched controls. Arthritis Rheum. 2003; 48:2178–2187. [PubMed: 12905471]
8. Scotti C, Hirschmann MT, Antinolfi P, et al. Meniscus repair and regeneration: review on current methods and research potential. Eur Cell Mater. 2013; 26:150–170. [PubMed: 24057873]
9. Lee AS, Kang RW, Kroin E, et al. Allograft meniscus transplatation. Sports Med Arthrosc. 2012; 20:106–114. [PubMed: 22555208]
10. Liu C, Toma I, Mastrogiacomo M, et al. Meniscus reconstruction: today's achievements and premises for the future. Arch Orthop Trauma Surg. 2013; 133:95–109. [PubMed: 23076654]
11. Sweigart MA, Athanasiou KA. Toward tissue engineering of the knee meniscus. Tissue Eng. 2001; 7:111–129. [PubMed: 11304448]
12. Heijkants RG, van Calck RV, De Groot JH, et al. Design, synthesis and properties of a degradable polyurethane scaffold for meniscus regeneration. J Mater Sci Mater Med. 2004; 15:423–427. [PubMed: 15332611]
13. Kobayashi M, Chang YS, Oka M. A two year in vivo study of polyvinyl alcohol-hydrogel (PVA-H) artificial meniscus. Biomaterials. 2005; 26:3243–3248. [PubMed: 15603819]
14. Cook JL, Fox DB, Malaviya P, et al. Long-term outcome for large meniscal defects treated with small intestinal submucosa in a dog model. Am J Sports Med. 2006; 34:32–42. [PubMed: 16157845]
15. Baker BM, Mauck RL. The effect of nanofiber alignment on the maturation of engineered meniscus constructs. Biomaterials. 2007; 28:1967–1977. [PubMed: 17250888]
16. Ionescu LC, Mauck RL. Porosity and cell preseeding influence electrospun scaffold maturation and meniscus integration in vitro. Tissue Eng Part A. 2013; 19:538–547. [PubMed: 22994398]
17. Kumbar SG, James R, Nukavarapu SP, et al. Electrospun nanofiber scaffolds: engineering soft tissues. Biomed Mater. 2008; 3:034002. [PubMed: 18689924]
18. Platt MA. Tendon repair and healing. Clin Podiatr Med Surg. 2005; 22:553–560. [PubMed: 16213379]
19. Gloria A, De Santis R, Ambrosio L. Polymer-based composite scaffolds for tissue engineering. J Appl Biomater Biomech. 2010; 8:57–67. [PubMed: 20740467]
20. Athanassiou K, Agrawal C, Barber F, et al. Orthopaedic applications for PLA–PGA biodegradable polymers. Arthroscopy. 1998; 14:726–737. [PubMed: 9788368]
21. Barber FA. Meniscus repair aftercare. Sports Med Arthrosc. 1999; 7:43–47.
22. Arnoczky SP, Lavagnino M. Tensile fixation of absorbable meniscal repair devices as a function of hydrolysis time. Am J Sports Med. 2001; 29:118–123. [PubMed: 11292034]
23. Asik M, Atalar AC. Failed resorption of bioabsorbable meniscus repair devices. Knee Surg Sports Traumatol Arthrosc. 2002; 10:300–304. [PubMed: 12355305]
24. Becker R, Schroder M, Starke C, et al. Biomechanical investigations of different meniscal repair implants in comparison with horizontal sutures on human meniscus. Arthroscopy. 2001; 17:439–444. [PubMed: 11337709]
25. Athanasiou KA, Niederauer GG, Agrawal CM. Sterilization, toxicit, biocompatibility and clinical applications of polylactic acid/polyglycolic acid copolymers. Biomaterials. 1996; 17:93–102. [PubMed: 8624401]

26. Oksman K, Skrifvars M, Selin JF. Natural fibres as reinforcement in polylactic acid (PLA) composites. Compos Sci Technol. 2003; 63:1317–1324.
27. Petersen W, Tillmann B. Collagenous fibril texture of the human knee joint menisci. Anat Embryol. 1998; 197:317–324. [PubMed: 9565324]
28. Pauli C, Grogan SP, Patil S, et al. Macroscopic and histopathologic analysis of human knee menisci in aging and osteoarthritis. Osteoarthr Cartil. 2011; 19:1132–1141. [PubMed: 21683797]
29. Barbero A, Grogan S, Schäfer D, et al. Age related changes in human articular chondrocyte yield, proliferation and post-expansion chondrogenic capacity. Osteoarthritis Cartilage. 2004; 12:476–484. [PubMed: 15135144]
30. Grogan SP, Aklin B, Frenz M, et al. In vitro model for the study of necrosis and apoptosis in native cartilage. J Pathol. 2002; 198:5–13. [PubMed: 12210057]
31. Roberts S, Menage J, Sandell LJ, et al. Immunohistochemical study of collagen types I and II and procollagen IIA in human cartilage repair tissue following autologous chondrocyte implantation. Knee. 2009; 16:398–404. [PubMed: 19269183]
32. Grogan SP, Miyaki S, Asahara H, et al. Mesenchymal progenitor cell markers in human articular cartilage: normal distribution and changes in osteoarthritis. Arthritis Res Ther. 2009; 11:R85. [PubMed: 19500336]
33. Martin I, Jakob M, Schäfer D, et al. Quantitative analysis of gene expression in human articular cartilage from normal and osteoarthritic joints. Osteoarthritis Cartilage. 2001; 9:112–118. [PubMed: 11237658]
34. Baker BM, Handorf AM, Ionescu LC, et al. New directions in nanofibrous scaffolds for soft tissue engineering and regeneration. Expert Rev Med Devices. 2009; 6:515–532. [PubMed: 19751124]
35. Li WJ, Mauck RL, Cooper JA, et al. Engineering controllable anisotropy in electrospun biodegradable nanofibrous scaffolds for musculoskeletal tissue engineering. J Biomech. 2007; 40:1686–1693. [PubMed: 17056048]
36. Metter RB, Ifkovits JL, Hou K, et al. Biodegradable fibrous scaffolds with diverse properties by electrospinning candidates from a combinatorial macromer library. Acta Biomater. 2010; 6:1219–1226. [PubMed: 19853066]
37. Nerurkar NL, Elliott DM, Mauck RL. Mechanics of oriented electrospun nanofibrous scaffolds for annulus fibrosus tissue engineering. J Orthop Res. 2007; 25:1018–1028. [PubMed: 17457824]
38. McCullen SD, Stevens DR, Roberts WA, et al. Characterization of electrospun nanocomposite scaffolds and biocompatibility with adipose- derived human mesenchymal stem cells. Int J Nanomedicine. 2007; 2:253–263. [PubMed: 17722553]
39. Deitzel JM, Kleinmeyer J, Harris D, et al. The effect of processing variables on the morphology of electrospun nanofibers and textiles. Polymer. 2001; 42:261–272.
40. Li W-J, Jiang YJ, Tuan RS. Chondrocyte phenotype in engineered fibrous matrix is regulated by fiber size. Tissue Eng. 2006; 12:1775–1785. [PubMed: 16889508]
41. Grogan SP, Chung PH, Soman P, et al. Digital micromirror device projection printing system for meniscus tissue engineering. Acta Biomater. 2013; 9:7218–7226. [PubMed: 23523536]
42. Mandal BB, Park SH, Gil ES, et al. Multilayered silk scaffolds for meniscus tissue engineering. Biomaterials. 2011; 32:639–651. [PubMed: 20926132]
43. Lannutti J, Reneker D, Ma T, et al. Electrospinning for tissue engineering scaffolds. Mater Sci Eng C Mater Biol Appl. 2007; 27:504–509.
44. Kai D, Prabhakaran MP, Stahl B, et al. Mechanical properties and in vitro behavior of nanofiber-hydrogel composites for tissue engineering applications. Nanotechnology. 2012; 23:095705. [PubMed: 22322583]
45. Han N, Johnson JK, Bradley PA, et al. Cell attachment to hydrogel-electrospun fiber mat composite materials. J Funct Biomater. 2012; 3:497–513. [PubMed: 24955629]
46. Xu T, Binder KW, Albanna MZ, et al. Hybrid printing of mechanically and biologically improved constructs for cartilage tissue engineering applications. Biofabrication. 2013; 5:015001. [PubMed: 23172542]

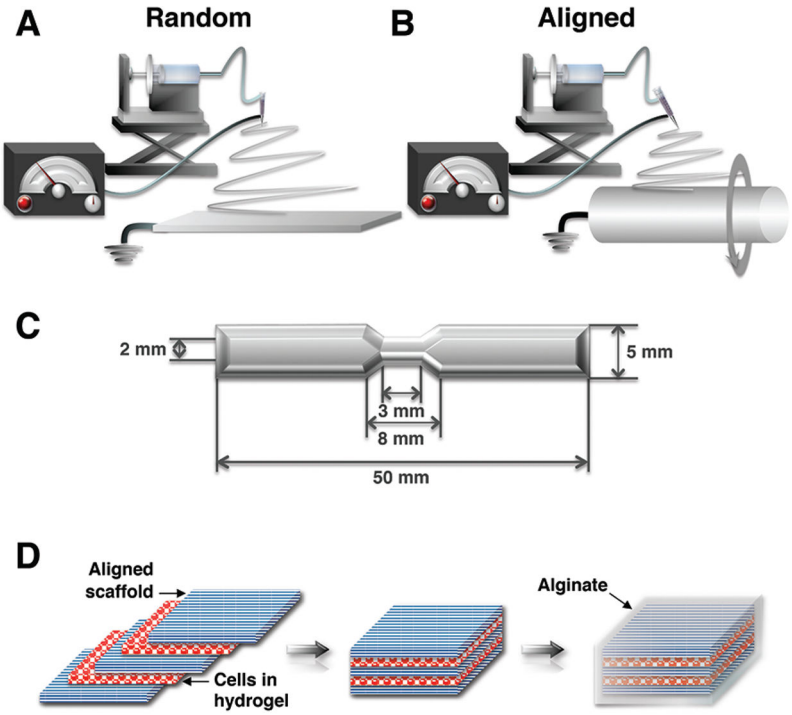

Figure 1. Overview of the electrospinning equipment and production of multiple layers

(A) A grounded plate collector produced random PLA fibers and (B) a rotating drum collector was used to deposit aligned PLA fibers. (C) Process of production of multiple layers. Human meniscus cells encapsulated in a hydrogel consisting of collagen type II, chondroitin sulfate and hyaluronan were seeded onto a base aligned PLA scaffold, followed by placement of another scaffold above in the same fiber orientation. This was followed by another layer of cells and one more scaffold layer. To hold the layers together, a layer of 2% alginate was deposited over the entire stack and crosslinked. (D) Geometry and size (mm) of the dog-bone shaped tensile test specimens.

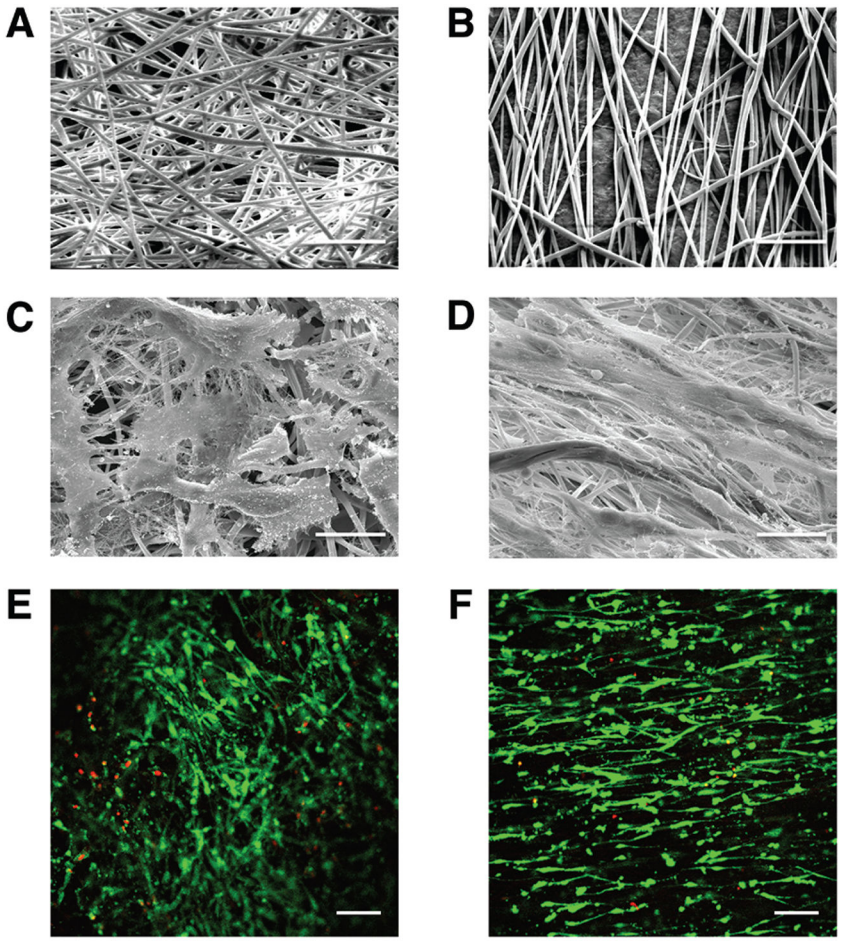

Figure 2. Scanning electron micrographs (SEM) of electrospun (ES) PLA scaffolds and cellular response

(A) SEM of random and (B) aligned ES PLA fibers (Mag. 1250×). (C) SEM of avascular human meniscus cells cultivated on random and (D) vascular human meniscus cells seeded on aligned ES PLA fibers (Mag. 1250×), scale bar: 20 μm in SEM images. (E) Confocal microscopy of vascular human meniscus cells cultured on random scaffolds and (F) avascular human meniscus cells cultivated on aligned scaffolds demonstrating viability (live/dead) and alignment cells cultivated on PLA scaffolds (Mag. 10×; scale bar: 200 μm in confocal images).

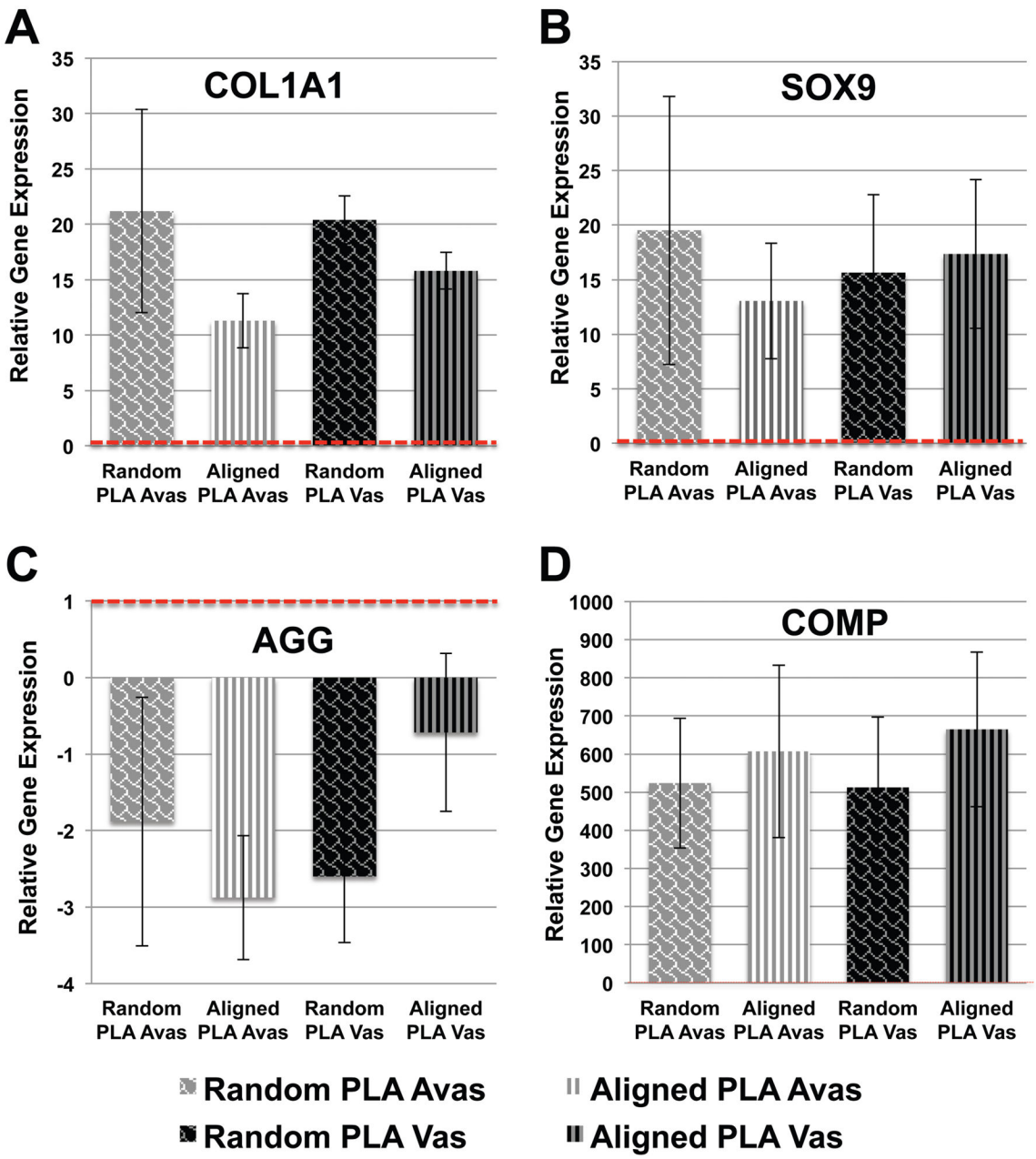

Figure 3. Relative fold change in gene expression of human vascular and avascular meniscus cells cultivated on either random or aligned PLA electrospun scaffolds

(A) Increased COL1A1 gene expression. (B) Increased SOX9 gene expression. (C) Reduced Aggrecan expression relative to monolayer controls. (D) COMP expression on random and aligned PLA electrospun scaffolds (n = 4–5 donors). Expression levels are relative to monolayer controls (dotted line).

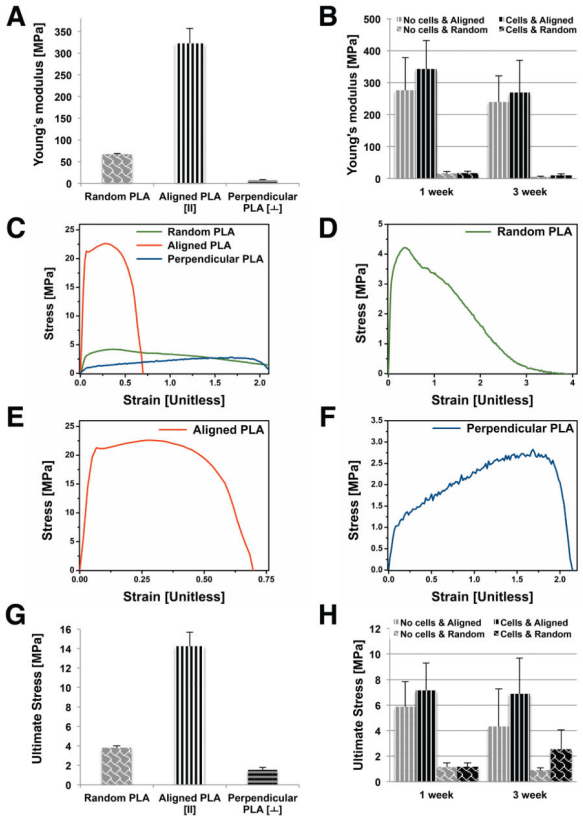

Figure 4. Mechanical testing of random and aligned ES PLA scaffolds

(A) Young's modulus (MPa) for random, aligned (along fiber orientation), and perpendicular to fiber orientation. (B) Young's modulus (MPa) of random & aligned electrospun PLA scaffolds over time in culture with or without cells (one week and three weeks). (C) Stress/strain curve for each condition and (D) random PLA scaffold. (E) aligned PLA scaffold (F) perpendicular oriented PLA scaffold. (G) Ultimate stress readings (MPa) for each condition. (H) Ultimate stress (MPa) for random & aligned electrospun PLA scaffolds over time in culture with or without cells (one week and three weeks).

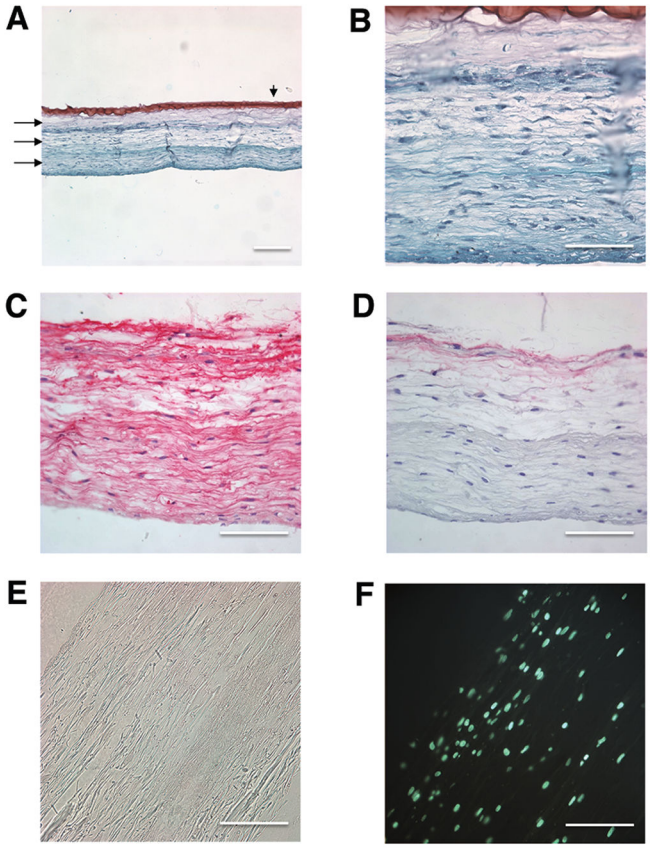

Figure 5. Histology and immunohistochemistry of multi-layer aligned PLA cell seeded scaffolds

(A–B) Safranin O/Fast-green stain. Arrows indicate three aligned PLA scaffold layers and the arrowhead points to the layer of alginate. (C) Collagen type I immunostain. (D) Isotype control stain. (E) Light microscope image of two weeks cultured construct. (F) DAPI stain. (Mag. A = 10×, scale bar: 200 μm ; Mag. B, C, D, E, and F = 40×, scale bar: 100 μm).